

Topological Insulators in Ternary Compounds with a Honeycomb Lattice

Hai-Jun Zhang¹, Stanislav Chadov², Lukas Müchler², Binghai Yan¹,
Xiao-Liang Qi¹, Jürgen Kübler³, Shou-Cheng Zhang¹, Claudia Felser^{1,2}

¹*Department of Physics, McCullough Building, Stanford University, Stanford, California 94305-404531*

²*Institut für Anorganische Chemie und Analytische Chemie,
Johannes Gutenberg - Universität, 55099 Mainz, Germany,*

³*Institut für Festkörperphysik, Technische Universität Darmstadt, 64289 Darmstadt, Germany **

(Dated: October 12, 2010)

One of the most exciting subjects in solid state physics is a single layer of graphite which exhibits a variety of unconventional novel properties. The key feature of its electronic structure are linear dispersive bands which cross in a single point at the Fermi energy. This so-called Dirac cone is closely related to the surface states of the recently discovered topological insulators. The ternary compounds, such as LiAuSe and KHgSb with a honeycomb structure of their Au-Se and Hg-Sb layers feature band inversion very similar to HgTe which is a strong precondition for existence of the topological surface states. In contrast to graphene with two Dirac cones at K and K' points, these materials exhibit the surface states formed by only a single Dirac cone at the Γ point together with the small direct band gap opened by a strong spin-orbit coupling (SOC) in the bulk. These materials are centro-symmetric, therefore, it is possible to determine the parity of their wave functions, and hence, their topological character. Surprisingly, the compound KHgSb with the strong SOC is topologically trivial, whereas LiAuSe is found to be a topological non-trivial insulator.

PACS numbers: 71.20.-b, 73.43.-f, 73.20.-r

Keywords: spin Hall effect, topological insulators

The search for new materials with inverted band structure provides the basis for the Quantum Spin Hall effect (QSH)[1–13]. This new exciting field started with the prediction and experimental observation of the QSH in quantum wells in two-dimensional topological insulator of the binary semiconductor HgTe [1, 2]. In a series of single crystals, such as Bi₂Se₃, three-dimensional topological insulating behavior was observed in topological surface states appearing as Dirac cones [7–9]. Later on, the manifold of Heusler semiconductors with 18 valence electrons and a similar band inversion was proposed [10, 11]. Since this proposed class of materials is extremely rich, it provides much wider flexibility in design by tuning the band gap size and the spin-orbit coupling (SOC) magnitude. In addition, the multi-functionality allows the incorporation of new properties such as superconductivity or magnetism [10].

The structure of the XYZ Heusler compounds can be simply viewed as “stuffed” YZ-zinc-blende. Depending on the stuffing element X Heuslers are semiconducting or semi-metallic [14]. Materials like ScPtBi are topologically similar to HgTe: the inversion of the conduction and valence bands occurs due to small electronegativity differences. Since HgTe and ScPtBi are both 2D topological insulators, the QSH is also expected in the corresponding quantum wells, as e.g. ScPtSb/ScPtBi, in full analogy to CdTe/HgTe. We emphasize that the check of parity at the time reversal points, as a sufficient condition for their topological character, is not possible here because of the absence of inversion symmetry [3].

Heusler compounds are similar to a stuffed diamond, correspondingly, it should be possible to find the “high Z” equivalent of graphene in a graphite-like structure with 18 valence electrons and with inverted bands. In this structure type with a lower symmetry compared to diamond three-dimensional topological behavior is realizable. Indeed, the honeycombs KZnP and KHgSb, crystallizing in so-called AlB₂, Ni₂In or ZrBeSi structure types, exhibit band ordering similar to the cubic CdTe and HgTe. However, in contrast to graphene, these compounds have a strong SOC which leads to a finite band gap at the Γ point [15, 16]. The determination of the wave function parity at the time-reversal points for these materials [3] is now possible, since they are centro-symmetric.

In detail, KHgSb, for instance, can be presented as a stuffed graphene in the following way: the electropositive K⁺ is stuffed in a honeycomb lattice of [HgSb]⁻ [17]. The ZrBeSi structure with additional stuffing electropositive main group elements is illustrated in Figure 1. One sees that the main group and the transition elements alternate within the same layer and between the layers, therefore the primitive unit cell consists of two formula units.

The number of ternary compounds crystallizing in this structure is nearly as large as in the Heusler family, however due to a weaker mean hybridization (sp^2 versus sp^3) many of the 18 valence electron compounds exhibit substantially smaller gaps or are simply metallic. As we show in the following, a certain number of semiconducting materials of this family with ordinary and inverted band structures can be found. In contrast to HgTe and ScPtBi, such materials with inverted structure exhibit real band gaps due to their higher structural anisotropy. For this reason the honeycomb compounds are three di-

* felser@uni-mainz.de

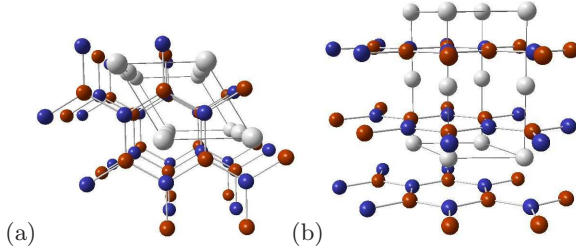


FIG. 1. (color online) Structure of KZnP, KHgSb, KCuSe and LiAuTe (ZrBeSi structure type) (a) shown in the $a-b$ plane and (b) along the c axis. Thus, the ternary semiconductor (with 18 valence electrons) can be viewed as stuffed relative of graphite with the honeycomb lattice consisting of alternating late transition metals (Ag, Au, Zn, Hg) and main group elements (Se, Te, P, As, Sb).

dimensional (3D), rather than 2D topological insulators. The 3D topological insulators exhibit an insulating energy gap in the bulk and gapless states on the surface protected by time-reversal symmetry [4]. These surface states exist only if there is an odd number of massless Dirac cones, with a single cone in the simplest case. The oddness is provided by the Z_2 topological invariant of the bulk [15, 18], thus any time-reversal invariant perturbation cannot open an insulating gap at the Dirac point on the surface.

The bulk band gap is defined by interplay of the lattice constant, spin-orbit coupling and the difference in electronegativities of the honeycomb sublattice constituents. In analogy to a ternary cubic semiconductors, new topological insulators can be found among the heavy 8/18 valence electron relatives of graphene, i.e. in a graphite XYZ structure type. Suitable atomic combinations are: (i) $X = \text{Li, Na, K, Rb, Cs}$; $Y = \text{Zn, Cd, Hg}$ and $Z = \text{P, As, Sb, Bi}$, or (ii) $X = \text{K, Rb, Cs}$; $Y = \text{Ag, Au}$ and $Z = \text{Se, Te}$, or (iii) $X = \text{rare earth}$, $Y = \text{Ni, Pd, Pt}$ and $Z = \text{P, As, Sb, Bi}$. Some of these combinations are not yet synthesized, some crystallize in different forms such as variants of the Cu₂Sb structure type (they will be the subject of another publication) and some, especially the rare earth containing compounds, are metallic. The known examples are KZnP, KZnSb, KZnAs, KHgAs, KHgSb, RbZnP, RbZnAs, RbZnSb, NaAuTe, KCuSe, KCuTe, KAuTe, and RbAuTe. Compounds such as LiAuSe, LiAuTe, CsAuTe, KHgBi, and CsHgBi are likely to be synthesized and we consider them in the present study as well. As mentioned above, the electronic structure of these materials is similar to their cubic analogues. The alkaline ions Li^+ , Na^+ , K^+ , Rb^+ , and Cs^+ “stuff” the graphite type YZ planar sublattice. Since these 18-electron compounds form such closed-shell structures, they are all non-magnetic and semiconducting. The difference is that in the case of binary semiconductors or C_{1b} Heuslers, the bonds within the YZ tetrahedrons are of sp^3 or sd^3 type, whereas in planar graphite-type layers the σ -type bonding occurs between the sp^2 or sd^2 orbitals. The remaining p -orbitals provide the π -type bonding interaction, similar

to graphite.

The search for the topological character of the proposed materials is based on *ab-initio* calculation of the electronic structure (for details see the supplemental). An important peculiarity of hexagonal systems is emphasized here: their unit cell consists of two formula units which results in a doubling of the corresponding bands. More details are given in the supplemental (Fig. 1) where it is seen that for KZnP (KHgSb) at the Γ point the doubled s -bands are split by about 10 meV. Thus for the weak coupling of the nearest honeycomb planes these doubled bands can become nearly indistinguishable. In the following we show that such doubling of the unit cell leads to a change of topology. Fortunately, the centro-symmetric space group (194) of the honeycomb-type compounds allows to make use of the parity eigenvalues [3, 8]. All relevant properties, i.e. the wave function parity in time-reversal symmetric k -points ($\Gamma(0,0,0)$, $M(\pi,0,0)$, $L(\pi,0,\pi)$, $A(0,0,\pi)$), the Z_2 invariant, the average nuclear charge $\langle Z \rangle$, the band gap width E_g and corresponding lattice parameters are listed in Table I for the compounds studied here.

TABLE I. Wave function parities at the time-reversal points, Z_2 topological invariant [3], average nuclear charge $\langle Z \rangle$, band gap E_g and optimized lattice parameters.

	Γ	M	L	A	Z_2	$\langle Z \rangle$	E_g [meV]	a [au]	c/a
LiAgSe	+	-	-	-	1	28	1	8.507	1.512
LiAgTe	-	-	-	-	0	34	45	8.979	1.526
LiAuSe	+	-	-	-	1	38.(6)	50	8.353	1.670
LiAuTe	+	-	-	-	1	44.(6)	-	8.818	1.663
NaAgSe	+	-	+	+	1	30.(6)	10	8.544	1.737
NaAgTe	+	-	+	+	1	36.(6)	3	9.031	1.719
NaAuSe	+	-	+	+	1	41.(3)	15	8.427	1.855
NaAuTe	+	-	+	+	1	47.(3)	30	8.894	1.823
KAgSe	-	-	+	+	0	33.(3)	15	8.836	1.989
KAgTe	-	-	+	+	0	39.(3)	230	9.193	1.958
KAuSe	-	-	+	+	0	44	20	8.742	2.077
KAuTe	+	-	+	+	1	50	-	8.780	2.097
LiZnAs	-	-	-	-	0	22	280	7.881	1.791
LiZnSb	-	-	-	-	0	28	10	14.121	1.762
LiHgAs	+	-	-	-	1	38.(6)	-	8.542	1.686
LiHgSb	+	-	-	-	1	44.(6)	-	9.070	1.665
NaZnAs	-	-	+	+	0	24.(6)	80	7.952	2.083
NaZnSb	-	-	+	+	0	30.(6)	230	8.539	2.007
NaHgAs	-	-	+	+	0	41.(3)	-	8.615	1.897
NaHgSb	-	-	+	+	0	47.(3)	140	9.148	1.845
KZnP	-	-	+	+	0	27.(3)	160	7.993	2.419
KZnSb	-	-	+	+	0	33.(3)	130	8.654	2.349
KHgAs	-	-	+	+	0	44	80	8.515	2.214
KHgSb	-	-	+	+	0	50	250	9.040	2.140

From previous studies on binary and ternary cubic

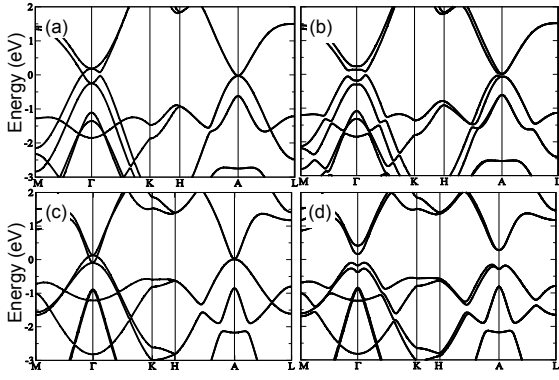


FIG. 2. Band structure of LiAuSe (a, b) and KHgSb (c, d) calculated without (a, c) and with (b, d) SOC.

semiconductors [10] it follows that it is more probable to find the $Z_2 = 1$ topological insulator among heavier compounds (with stronger SOC). Indeed, their bands splitting scales roughly with the average nuclear charge $\langle Z \rangle = 1/N \sum_{i=1}^N Z_i$ where $N = 2$ for binaries and $N = 3$ for ternaries. This parameter sorts cubic systems almost along a straight line [10]. However Table I clearly illustrates that this does not hold for the semiconductors of the ZrBeSi structure type. Indeed, only Lithium compounds within the Zn and Hg group show the expected trend. The compounds with Zn are topologically trivial whereas those with Hg are non-trivial insulators. Compounds with heavier alkaline metals (Na, K) are all trivial independently of whether or not they contain Zn or Hg. Among the Ag- and Au-containing compounds more non-trivial systems are found, however the correlation between band inversion and $\langle Z \rangle$, as in the cubic semiconductors, is absent. For example, the topological insulator LiAgSe corresponds to $\langle Z \rangle = 28$, whereas for the topologically trivial KHgSb system $\langle Z \rangle = 50$.

In Figure 2 the band structure of LiAuSe (upper panel) is compared with KHgSb (lower panel) calculated at time-reversal symmetric points with (right) and without (left) SOC. It follows that both compounds are semimetals with degeneracies at the Γ and A symmetry points if SOC is omitted. The degenerate p_x and p_y states mediate σ -type Sb/Se and Hg/Au bonding. The lower-lying Hg/Au bands are of s type, similar to HgTe. Inclusion of SOC opens a band gap at the Fermi energy at the Γ and A points leading to the typical dips in the band structure for both compounds [19]. The resulting parities for both materials listed in Table I match only at the M point, whereas at Γ , A , and L they differ, leading to a trivial state in KHgSb and topological insulator in LiAuSe.

To understand the mechanisms of the band inversion and parity change in details one can track the band structure evolution near the Γ point by starting from the simple atomic energy levels and subsequently introducing chemical bonding (step I), crystal field (II), and SOC (III). The resulting changes are schematically shown in Fig. 3. As an example we took the KZnP sys-

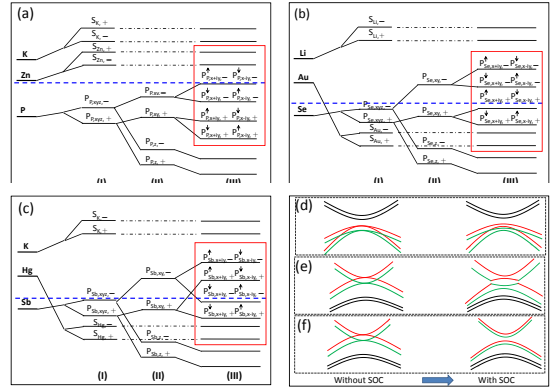


FIG. 3. (Color online) The structure of the atomic orbitals. (a) Evolution of atomic orbitals at the Γ point in KZnP system, which has no inverted bands formed by Zn s and P $p_{x,y,z}$ -orbitals. Steps (I-III) represent the effect of turning on chemical bonding (I), crystal-field splitting (II) and SOC (III). The blue dashed line marks the Fermi energy. Similar scheme for LiAuSe (b) and KHgSb (c), (d), (e) and (f) represent the schematic band structure for KZnP, LiAuSe and KHgSb near the Γ point, respectively. The black curves mark the orbitals with mainly Zn (or Au and Hg) s -character, red and green curves are the rest of light and heavy hole-like bands.

tem. The low-lying $3s$ -orbital of $P(3s^23p^3)$ can be neglected and the consideration can be restricted to the s -orbitals of $K(4s)$ and $Zn(3d^{10}4s^2)$ and the $p_{x,y,z}$ orbitals of $P(3s^23p^3)$. In step I the chemical bonding is introduced. It is convenient to make use of the inversion symmetry and recombine the orbitals according to their parities. K and Zn give two even and two odd s -orbitals $|S_{K,\pm}\rangle$, $|S_{Zn,\pm}\rangle$; P gives three odd and three even p -orbitals $|P_{P,xyz,\pm}\rangle$, where “ \pm ” are the parity labels. In step II the crystal field is switched on which splits the $|P_{P,xyz,\pm}\rangle$ into $|P_{P,xy,\pm}\rangle$ and $|P_{P,z,\pm}\rangle$ according to the hexagonal symmetry. In step III the SOC is turned on. This leads to a splitting between $|P_{P,x+iy,-\downarrow(\uparrow)}\rangle$ and $|P_{P,z,\pm,\uparrow(\downarrow)}\rangle$ orbitals. The Fermi level falls into the middle of $|P_{P,x+iy,-\downarrow}\rangle$ (or $|P_{P,x-iy,-\uparrow}\rangle$) and $|P_{P,x+iy,+,\uparrow}\rangle$ (or $|P_{P,x-iy,+,\downarrow}\rangle$) as shown in Figure 3 (a). No inversion occurs between the s -orbital of K (or Zn) and p -orbital of P , similar to the CdTe case. However, this situation changes for the LiAuSe and KHgSb compounds. Due to the very delocalized character of Au (Hg) d -orbitals the s -orbital of Li (K) is pulled down below the p -orbital of P , which leads to band inversion similar to the HgTe case [20]. The corresponding evolution for LiAuSe and KHgSb is shown in Figures 3 (b) and (c). In addition, $|P_{Sb,x+iy,-,\downarrow}\rangle$ (or $|P_{Sb,x-iy,-,\uparrow}\rangle$) and $|P_{Sb,x+iy,+,\uparrow}\rangle$ (or $|P_{Sb,x-iy,+,\downarrow}\rangle$) are inverted because of the strong SOC in KHgSb. We emphasize that since there are two band inversions occurring in KHgSb it becomes topologically trivial. In contrast, LiAuSe exhibits inversion only between the s - and p -orbitals since its SOC is too weak to invert $|P_{Sb,x+iy,-,\downarrow}\rangle$ (or $|P_{Sb,x-iy,-,\uparrow}\rangle$) and $|P_{Sb,x+iy,+,\uparrow}\rangle$ (or $|P_{Sb,x-iy,+,\downarrow}\rangle$). Thus we conclude that LiAuSe is topologically non-trivial. The corresponding band struc-

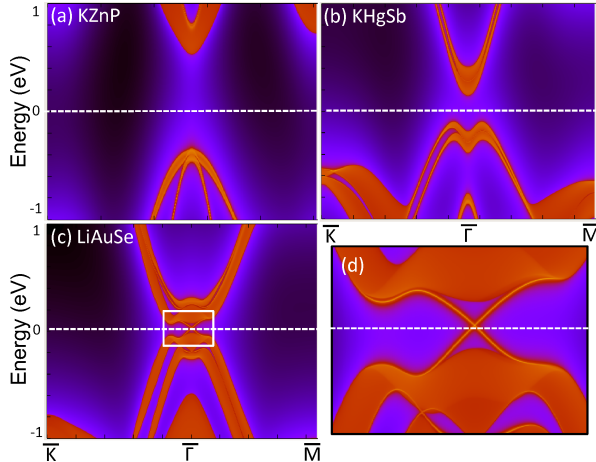


FIG. 4. (color online) The band structure of the semi-infinite (vacuum/solid-interface) corresponding to (a) trivial KZnP, (b) non-trivial LiAuSe and (c) trivial KHgSb insulators, calculated along the $\bar{K}-\bar{\Gamma}-\bar{M}$ directions of the Brillouin zone. In contrast to KZnP and KHgSb, LiAuSe exhibits the surface states seen in the bulk energy gap (zoomed in the inset (d)).

tures around the Γ point for KZnP, LiAuSe and KHgSb are shown schematically in Figures 3 (d-f). It is seen that in KZnP no band inversion occurs, in LiAuSe it occurs once and KHgSb twice.

For the final test of the topological/trivial character we directly calculate the surface states of the proposed systems. The electronic structure of the surface can be adequately described by the vacuum/solid interface within a unit cell which is sufficiently large along a certain direction. By utilizing the so-called decimation technique [21] such a unit cell can be extended to infinity which ensures

correct boundary conditions. Such calculations typically require a formalism using fast decaying basis functions. In the present work we apply the Wannier functions approach [22]. As it follows from the band structures shown in Figure 4 only LiAuSe exhibits gapless surface states seen as a single Dirac cone within the bulk energy gap at the Γ point. The estimate of its Fermi velocity gives about 1.8×10^5 m/s which is smaller than that for Bi_2Se_3 . In contrast, KZnP and KHgSb remain insulators at the surface. Thus the surface state calculation agrees with the bulk parity analysis and conclusively confirms the existence of the topologically non-trivial materials within proposed honeycomb type structure.

In conclusion we emphasize that topologically non-trivial systems can be found in the proposed class of honeycomb structure semiconductors. The interplay of mechanisms which are responsible for the topologically trivial or non-trivial character in these systems differs from the cubic semiconductors studied earlier. In particular it is shown that the strong SOC and weak inter-layer coupling causes a double inversion which in turn makes the compound trivial. In contrast to the topologically non-trivial cubic systems which exhibit a zero band gap in the bulk, the topologically non-trivial hexagonal materials provide the “natural” 3D topological materials with a real bulk band gap and gapless states at the surface.

ACKNOWLEDGMENTS

The work was supported by the supercomputing center at Stanford Institute Materials and Energy Science. The financial support of the DFG/ASPIMATT project (unit 1.2-A) is gratefully acknowledged.

-
- [1] B. A. Bernevig, T. L. Hughes, and S. C. Zhang, *Science* **314**, 1757 (2006).
 - [2] M. König, S. Wiedmann, C. Brüne, A. Roth, H. Buhmann, L. Molenkamp, X. L. Qi, and S. C. Zhang, *Science* **318**, 766 (2007).
 - [3] L. Fu and C. L. Kane, *Phys. Rev. B* **76**, 045302 (2007).
 - [4] L. Fu, C. L. Kane, and E. J. Mele, *Phys. Rev. Letters* **98**, 106803 (2007).
 - [5] X. Dai, T. L. Hughes, X.-L. Qi, Z. Fang, and S.-C. Zhang, *Phys. Rev. B* **77**, 125319 (2008).
 - [6] D. Hsieh, D. Qian, L. Wray, Y. Xia, Y. S. Hor, R. J. Cava, and M. Z. Hasan, *Nature* **452**, 970 (2008).
 - [7] Y. Xia, D. Qian, D. Hsieh, L. Wray, A. Pal, H. Lin, A. Bansil, D. Grauer, Y. S. Hor, R. J. Cava, and M. Z. Hasan, *Nature Physics* **5**, 398 (2009).
 - [8] H. Zhang, C.-X. Liu, X.-L. Qi, X. Dai, Z. Fang, and S. C. Zhang, *Nature Physics* **5**, 438 (2009).
 - [9] Y. L. Chen, J. G. Analyti, J. H. Chu, Z. K. Liu, S. K. Mu, X. L. Qi, H. J. Zhang, D. H. Lu, X. Dai, Z. Fang, S. C. Zhang, I. R. Fisher, Z. Hussain, and Z. X. Shen, *Science* **325**, 178 (2009).
 - [10] S. Chadov, X.-L. Qi, J. Kübler, G. H. Fecher, C. Felser, and S.-C. Zhang, *Nature Materials* **9**, 541 (2010).
 - [11] H. Lin, L. A. Wray, Y. Xia, S. Xu, S. Jia, R. J. Cava, A. Bansil, and M. Z. Hasan, *Nature Materials* **9**, 546 (2010).
 - [12] X.-L. Qi and S.-C. Zhang, *Physics Today* **63**, 33 (2010).
 - [13] J. Moore, *Nature* **464**, 194 (2010).
 - [14] H. C. Kandpal, C. Felser, and R. Seshadri, *J. Phys. D: Appl. Phys.* **39**, 776 (2006).
 - [15] C. L. Kane and E. J. Mele, *Phys. Rev. Letters* **95**, 226801 (2005).
 - [16] B. A. Bernevig and S. C. Zhang, *Phys. Rev. Letters* **96**, 106802 (2006).
 - [17] F. Casper, C. Felser, R. Seshadri, P. Sebastian, and R. Pöttgen, *J. Phys. D: Appl. Phys.* **41**, 035002 (2008).
 - [18] C. L. Kane and E. J. Mele, *Phys. Rev. Letters* **95**, 146802 (2005).
 - [19] M. Klintenberg, arXiv:1007.4838v1.
 - [20] A. Delin, *Phys. Rev. B* **65**, 153205 (2002).
 - [21] H.-J. Zhang, C.-X. Liu, X.-L. Qi, X.-Y. Deng, X. Dai, S.-C. Zhang, and Z. Fang, *Phys. Rev. B* **80**, 085307 (2009).
 - [22] I. Souza, N. Marzari, and D. Vanderbilt, *Phys. Rev. B* **65**, 035109 (2001).

Supplementary material: Topological Insulators in Ternary Compounds with a Honeycomb Lattice

Hai-Jun Zhang¹, Stanislav Chadov², Lukas Müchler², Binghai Yan¹,
Xiao-Liang Qi¹, Jürgen Kübler³, Shou-Cheng Zhang¹, Claudia Felser^{1,2}

¹*Department of Physics, McCullough Building, Stanford University, Stanford, California 94305-404531*

²*Institut für Anorganische Chemie und Analytische Chemie,
Johannes Gutenberg - Universität, 55099 Mainz, Germany,*

³*Institut für Festkörperphysik, Technische Universität Darmstadt, 64289 Darmstadt, Germany **

(Dated: October 12, 2010)

This is supplementary material. We provide the details of electronic structure calculation, parity definition and illustrate the analogy in the band structures of cubic and hexagonal semiconductors.

PACS numbers: 71.20.-b, 73.43.-f, 73.20.-r

Keywords: spin Hall effect, topological insulators

Calculation of the electronic structure is performed by the plane-wave based pseudopotential BSTATE (Beijing Simulation Tool of Atomic TEchnology) package [1]. The exchange-correlation potential is treated within the Generalized Gradient Approximation (GGA) [2]. The lattice parameters listed in present work are obtained by doing the *ab-initio* geometry optimization.

The topological character is calculated by following Ref. [3]. The central quantity here is the parity product $\delta_i = \prod_{m=1}^N \xi_{2m}(\Gamma_i)$, where N is the number of filled bands and $\xi_{2m}(\Gamma_i)$ is the parity eigenvalue of the $2m$ -th occupied band at the time reversal point Γ_i . The Z_2 invariant, $\nu_0 = 0$ or 1 , is then obtained from the product $(-1)^{\nu_0} = \prod_i \delta_i$.

Figure 1 illustrates the analogy between cubic C_{1b} compounds and hexagonal semiconductors, by compar-

ing the band structures of CdTe and HgTe with hexagonal ternaries KZnP and KHgSb. Clear fingerprints can immediately be identified: both CdTe and KZnP exhibit a direct gap at the Γ point formed by splitting of the conduction (*s*-type) and the valence (*p*-type) bands. By going from CdTe to HgTe and from KZnP to KHgP the bands at the Γ point invert in a similar manner: the *s*-type shifts below the *p*-type band. However, in contrast to HgTe and other C_{1b} Heuslers, the hexagonal symmetry with varying c/a ratios allows to lift the degeneracy of the *p*-type bands and opens a finite band gap. As we mentioned this suggests KHgSb and the related materials as candidates for a 3D topological insulators, similar to Bi_2Se_3 . It follows from the flat bands along the $K-H$ direction that the material is quasi two-dimensional which leads to a strong anisotropy of its transport properties.

-
- [1] Z. Fang and K. Terakura, J. Phys.: Condens. Matter **14**, 3001 (2002).
[2] J. P. Perdew, K. Burke, and M. Ernzerhof, Phys. Rev.

- Letters **77**, 3865 (1996).
[3] L. Fu and C. L. Kane, Phys. Rev. B **76**, 045302 (2007).

* felser@uni-mainz.de

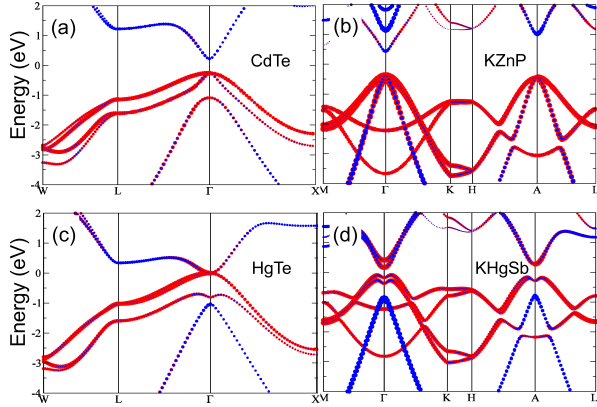


FIG. 1. (color online) Comparison of the band structures of cubic binaries (CdTe, HgTe) with hexagonal (KZnP, KHgSb) ternary compounds. In both CdTe and KZnP the valence and conduction bands are formed mainly by the p (red) and the s (blue) states, respectively.